

The ratio F_K/F_π in QCD

S. Dürr^{1,2}, Z. Fodor^{1,2,3}, C. Hoelbling¹, S. D. Katz^{1,3}, S. Krieg⁵, T. Kurth¹, L. Lellouch⁴,
T. Lippert^{1,2}, A. Ramos⁴, K. K. Szabó¹

[Budapest-Marseille-Wuppertal Collaboration]

¹*Bergische Universität Wuppertal, Gausstr. 20, D-42119 Wuppertal, Germany*

²*Jülich Supercomputing Center, Forschungszentrum Jülich, D-52425 Jülich, Germany*

³*Institute for Theoretical Physics, Eötvös University, H-1117 Budapest, Hungary*

⁴*Centre de Physique Théorique⁰, CNRS Luminy, Case 907, F-13288 Marseille Cedex 9, France*

⁵*Center for Theoretical Physics, MIT, Cambridge, MA 02139-4307, USA*

Abstract

We determine the ratio F_K/F_π in QCD with $N_f = 2 + 1$ flavors of sea quarks, based on a series of lattice calculations with three different lattice spacings, large volumes and a simulated pion mass reaching down to about 190 MeV. We obtain $F_K/F_\pi = 1.192(7)_{\text{stat}}(6)_{\text{syst}}$. This result is then used to give an updated value of the CKM matrix element $|V_{us}|$. The unitarity relation for the first row of this matrix is found to be well observed.

arXiv:1001.4692v1 [hep-lat] 26 Jan 2010

⁰Centre de Physique Théorique is “UMR 6207 du CNRS et des universités d’Aix-Marseille I, d’Aix-Marseille II et du Sud Toulon-Var, affiliée à la FRUMAM”.

1 Introduction

An accurate determination of the Cabibbo-Kobayashi-Maskawa (CKM) matrix element $|V_{us}|$ is important, because it allows to put bounds on possible extensions of the Standard Model of Particle Physics which, in turn, are relevant to guide direct searches, e.g. those planned at the Large Hadron Collider (LHC) at CERN [1].

Since the kaon is the lightest particle with strangeness, it is not surprising that much of the recent progress in this field derives from precision studies of leptonic and semi-leptonic decays of kaons (see e.g. [2]). The theoretical challenge is to link the experimentally observed branching fractions to fundamental parameters in the underlying theory, e.g. the CKM matrix elements in the Standard Model. In this step lattice QCD calculations can help by providing decay constants and transition form factors. For an overview on these activities see e.g. the summary talks on kaon physics at the last three lattice conferences [3, 4, 5].

In this paper we shall follow a proposal by Marciano [6] to derive $|V_{us}|$ from $|V_{ud}|$, using a lattice determination of the ratio F_K/F_π of leptonic decay constants. More specifically, in

$$\frac{\Gamma(K \rightarrow l\bar{\nu}_l)}{\Gamma(\pi \rightarrow l\bar{\nu}_l)} = \frac{|V_{us}|^2 F_K^2 M_K (1 - m_l^2/M_K^2)^2}{|V_{ud}|^2 F_\pi^2 M_\pi (1 - m_l^2/M_\pi^2)^2} \left\{ 1 + \frac{\alpha}{\pi} (C_K - C_\pi) \right\} \quad (1)$$

the l.h.s., even after dividing it by the radiative correction factor (the last bracket on the r.h.s.), is known to 0.4% precision, if $l = \mu$ is considered [7]. Also M_K , M_π and m_μ are known with a relative precision of $3 \cdot 10^{-5}$, $3 \cdot 10^{-6}$ and 10^{-7} , respectively [7]. And $|V_{ud}|$ has been determined from super-allowed nuclear β -decays with an accuracy better than 0.03% [7, 8]. Therefore, the limiting factor for a precise determination of $|V_{us}|$ via (1) is F_K/F_π – this ratio is typically determined with a precision of a few percent in present days lattice QCD studies.

Here we present a state-of-the art determination of F_K/F_π in QCD in which all sources of systematic uncertainty are properly taken into account. We have performed a series of dynamical lattice calculations with a degenerate up and down quark mass m_{ud} and a separate strange quark mass m_s , a scheme commonly referred to as $N_f = 2 + 1$. The strange quark mass is roughly held fixed close to its physical value ($m_s \simeq m_s^{\text{phys}}$), while the light quark mass is heavier than in the real world, but varied all the way down to values which make a controlled extrapolation to the physical mass possible. The spatial size L is chosen sufficiently large, such that the extracted F_K/F_π values can be corrected, by means of Chiral Perturbation Theory, for (small) finite-volume effects. Since our calculation includes three lattice spacings, a combined fit to all simulation results yields a controlled extrapolation to the continuum and to the physical mass point. Details of our action and algorithm have been specified in [9], where evidence for excellent scaling properties is also given.

This paper is organized as follows. Sec. 2 contains a survey of where our simulation points are located in the $(M_\pi^2, 2M_K^2 - M_\pi^2)$ plane, a discussion of which chiral extrapolation formulae might be appropriate, an account of our strategies to quantify (and correct for) cutoff and finite-volume effects, and a description of the overall fitting procedure that is used to determine F_K/F_π . In Sec. 3 the final result is given and compared to other unquenched calculations [10]-[18] of F_K/F_π . In Sec. 4 our result is converted, by means of (1), into a value for $|V_{us}|$. We find that, within errors, the first row unitarity relation $|V_{ud}|^2 + |V_{us}|^2 + |V_{ub}|^2 = 1$ is well observed. This, in turn, puts tight constraints on possible extensions of the Standard Model [1, 2].

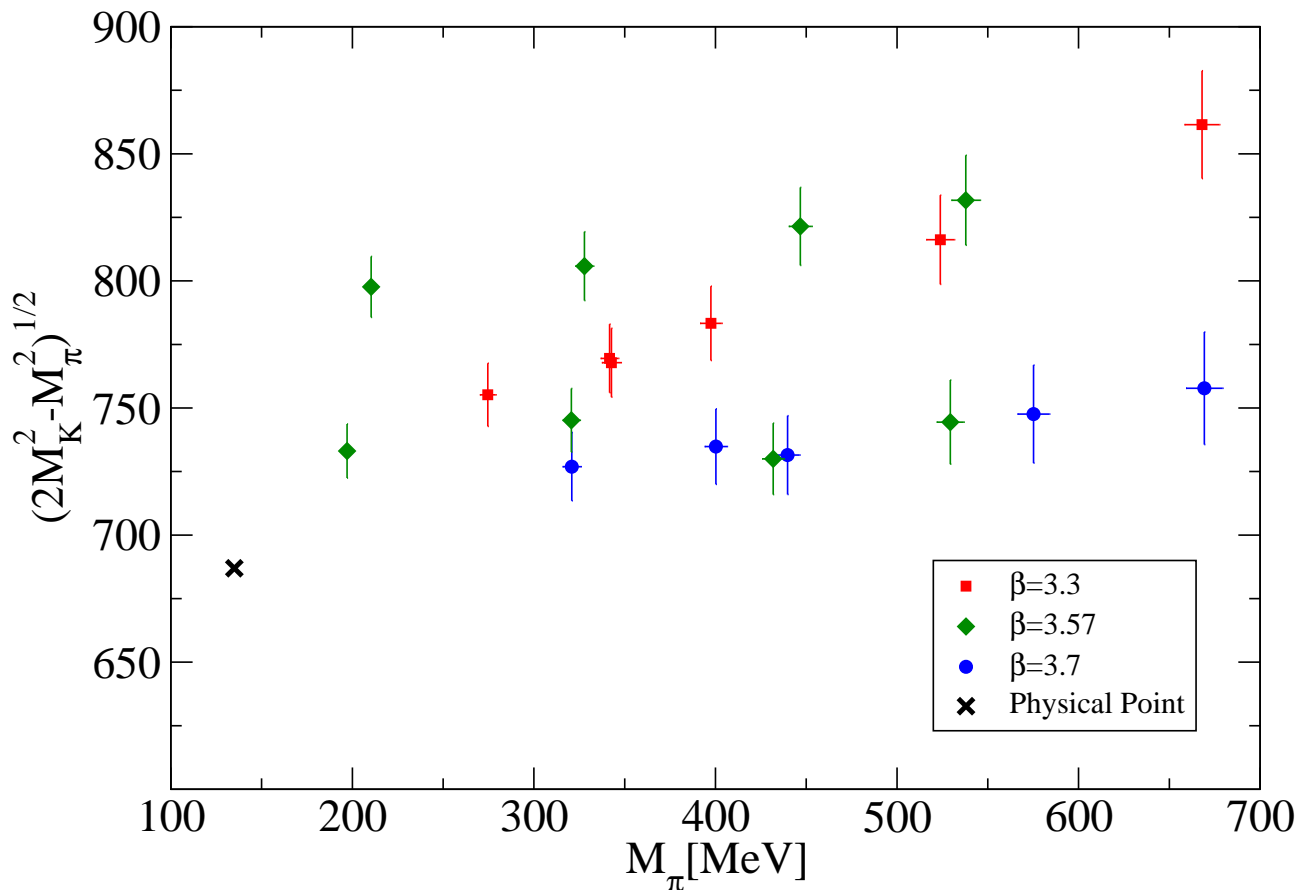


Figure 1: Overview of our simulation points in terms of M_π and $\sqrt{2M_K^2 - M_\pi^2}$. The former gives a measure of the isospin averaged up and down quark mass while the later determines the strange quark mass. The symbols refer to the three lattice spacings $a \simeq 0.124$ fm ($\beta = 3.3$), $a \simeq 0.083$ fm ($\beta = 3.57$), and $a \simeq 0.065$ fm ($\beta = 3.7$), respectively, and the physical point is marked with a cross. Error bars are statistical only. The numbers given correspond to one of the 18 two-point function, time fit-intervals that we use in our estimate of systematic uncertainties (see Sec. 2.5 for details). At $\beta = 3.3$ and $\beta = 3.7$ only a single value of the strange quark mass, close to the physical value, is considered. At $\beta = 3.57$, simulations are performed at three values of the strange quark mass (see text for details).

2 Simulation and analysis details

2.1 Simulation parameters

Our gauge and fermion actions, as well as details of the algorithm that is used to simulate QCD with $N_f = 2 + 1$ dynamical flavors, have been specified in [9]. Here, it is sufficient to say that our action combines good scaling properties with a one-to-one matching of lattice-to-continuum flavor; this avoids the complications of a low-energy theory with unphysical flavor symmetry breaking.

We adjust the quark masses m_{ud} , m_s and set the lattice spacing a using aM_π , aM_K and aM_Ξ . We adopt a mass independent scale setting scheme. This means that we extrapolate, for each coupling $\beta = 3.3, 3.57, 3.7$, the values aM_π, aM_K, aM_Ξ to the point where any two of

β	am_{ud}	am_s	$L^3 \times T$	traj.	aM_π	aM_K	F_K/F_π
3.3	-0.0960	-0.057	$16^3 \times 32$	10000	0.4115(6)	0.4749(6)	1.0474(5)
	-0.1100	-0.057	$16^3 \times 32$	1450	0.322(1)	0.422(1)	1.079(2)
	-0.1200	-0.057	$16^3 \times 64$	4500	0.2448(9)	0.3826(6)	1.113(3)
	-0.1233	-0.057	$24^3 \times 64$	2000	0.2105(8)	0.3668(6)	1.137(6)
	-0.1233	-0.057	$32^3 \times 64$	1300	0.211(1)	0.3663(8)	1.130(5)
	-0.1265	-0.057	$24^3 \times 64$	2100	0.169(1)	0.3500(7)	1.153(6)
3.57	-0.0318	0,-0.010	$24^3 \times 64$	1650,1650	0.2214(7),0.2178(5)	0.2883(7),0.2657(5)	1.085(1),1.057(1)
	-0.0380	0,-0.010	$24^3 \times 64$	1350,1550	0.1837(7),0.1778(7)	0.2720(6),0.2469(6)	1.107(3),1.092(2)
	-0.0440	0,-0.007	$32^3 \times 64$	1000,1000	0.1348(7),0.1320(7)	0.2531(6),0.2362(7)	1.154(4),1.132(4)
	-0.0483	0,-0.007	$48^3 \times 64$	500,1000	0.0865(8),0.0811(5)	0.2401(8),0.2210(5)	1.22(1),1.178(7)
3.7	-0.007	0.0	$32^3 \times 96$	1100	0.2130(4)	0.2275(4)	1.0223(4)
	-0.013	0.0	$32^3 \times 96$	1450	0.1830(4)	0.2123(3)	1.0476(9)
	-0.020	0.0	$32^3 \times 96$	2050	0.1399(3)	0.1920(3)	1.089(2)
	-0.022	0.0	$32^3 \times 96$	1350	0.1273(5)	0.1882(4)	1.102(2)
	-0.025	0.0	$40^3 \times 96$	1450	0.1021(4)	0.1788(4)	1.137(6)

Table 1: *Parameters and selected results from our simulations. The errors quoted here are purely statistical. These results correspond to one of the 18 two-point function, time fit-intervals that we use in our estimate of systematic uncertainties (see Sec. 2.5 for details). In this particular analysis, the scales at $\beta = 3.3, 3.57, 3.7$ are $a^{-1} = 1616(20)$ MeV, $2425(27)$ MeV, $3142(37)$ MeV, respectively.*

the ratios in $M_\pi/M_K/M_\Xi$ agree with their experimental values. Alternatively we have used Ω instead of Ξ to set the scale and used the difference between the two methods as an estimate of the systematics of scale fixing (see Sec. 2.5). Our simulations do not account for isospin breaking and electromagnetic interactions; thus experimental inputs need to be corrected for these effects. We use $M_\pi^{\text{phys}} = 135$ MeV, $M_K^{\text{phys}} = 495$ MeV, $M_\Xi^{\text{phys}} = 1318$ MeV and $M_\Omega^{\text{phys}} = 1672$ MeV with an error of a few MeV [11].

Using LO chiral perturbation theory as a guide, we fix the bare strange quark mass at a given β , such that the computed $2M_K^2 - M_\pi^2$ approaches its physical value when extrapolated in M_π^2 to the physical point. As Tab. 1 indicates and Fig. 1 illustrates, only one bare strange quark mass is used at $\beta=3.3$ and at $\beta=3.7$, and it is very near the value required to reach the physical point. At $\beta=3.57$, three values of the strange quark mass are considered to provide some lever arm for an interpolation to the physical m_s . The fact that our simulation points lie above the physical value of $2M_K^2 - M_\pi^2$ is due in part to cutoff effects in the relation of this quantity to the vector Ward identity strange quark mass. Indeed, for $\beta=3.3$ and 3.7 , $2M_K^2 - M_\pi^2$ extrapolates near its physical value at $M_\pi = M_\pi^{\text{phys}}$, and the slope with which it extrapolates tends to zero as β increases.

Regarding m_{ud} , we cover pion masses all the way down to ~ 190 MeV. On every ensemble the ratio F_K/F_π is measured with the valence up/down or strange quark mass set equal to the corresponding sea quark mass, so only the unitary theory is considered. Results are collected in Tab. 1. It is worth noting that this same dataset was successfully used to determine the light hadron spectrum [19].

We now give details of how we extrapolate to the physical mass point, to the continuum, and to infinite volume. We continue with an explanation of our global fitting strategy and the

pertinent assessment of systematic errors.

2.2 Extrapolation to the physical mass point

From the discussion above it is clear that we need to extrapolate our results for F_K/F_π in m_{ud} to m_{ud}^{phys} , while the strange quark mass is already close to m_s^{phys} . It is important to note that even the extrapolation in m_{ud} is small, amounting to only a couple percent in F_K/F_π . Thus, any reasonable, well-motivated functional form which fits our results with a good confidence level should give a reliable estimate of F_K/F_π at the physical point. In order to assess the theoretical error that arises in this extrapolation, we choose to invoke three frameworks to parameterize the quark mass dependence:

- (i) $SU(3)$ chiral perturbation theory (χ PT) [20],
- (ii) heavy kaon $SU(2)$ chiral perturbation theory [16],
- (iii) ‘‘Taylor’’ extrapolations involving polynomial ansaetze [4].

We now summarize the theoretical background of these functional forms.

Ad (i): $SU(3)$ χ PT assumes that the u , d and s quark masses are small compared to the scale of chiral symmetry breaking. At NLO, the ratio F_K/F_π can be written [20]

$$\frac{F_K}{F_\pi} = \frac{1 - \frac{1}{32\pi^2 F_0^2} \left\{ \frac{3}{4} M_\pi^2 \log\left(\frac{M_\pi^2}{\mu^2}\right) + \frac{3}{2} M_K^2 \log\left(\frac{M_K^2}{\mu^2}\right) + [M_K^2 - \frac{1}{4} M_\pi^2] \log\left(\frac{4M_K^2 - M_\pi^2}{3\mu^2}\right) \right\} + \frac{4}{F_0^2} M_K^2 L_5}{1 - \frac{1}{32\pi^2 F_0^2} \left\{ 2M_\pi^2 \log\left(\frac{M_\pi^2}{\mu^2}\right) + M_K^2 \log\left(\frac{M_K^2}{\mu^2}\right) \right\} + \frac{4}{F_0^2} M_\pi^2 L_5} \quad (2)$$

where, for $P = \pi, K, \eta$,

$$\mu_P = \frac{M_P^2}{32\pi^2 F_0^2} \log\left(\frac{M_P^2}{\mu^2}\right) \quad (3)$$

and where M_P , at this order, can be taken to be the lattice measured masses, with $M_\eta^2 \stackrel{\text{LO}}{=} (4M_K^2 - M_\pi^2)/3$, using the LO $SU(3)$ relation. Note that in obtaining (2), we have used the freedom to reshuffle subleading terms between numerator and denominator to cancel the sea quark contributions common to F_K and F_π , which are proportional to the low energy constant (LEC) L_4 . That leaves only one NLO LEC in (2), i.e. $L_5(\mu)$, whose μ dependence cancels the one in the logarithms. Throughout, we shall keep μ fixed to 770 MeV, the value which is customary in phenomenology.

In addition to Eq. (2), we consider two more $SU(3)$ χ PT expressions, which are equivalent to (2) at NLO: the one obtained by fully expanding (2) to NLO and the one obtained by expanding the inverse of (2) to NLO. The use of these three different forms is one of the ways that we have to estimate the possible contributions of higher order terms (see Sec. 2.5).

A number of collaborations have reported difficulties and large corrections when fitting their results for F_π and F_K to NLO $SU(3)$ chiral perturbation theory (or its partially quenched descendent) around $M_\pi \gtrsim 400$ MeV [4]. This suggests that m_s^{phys} might be the upper end of the quark mass range where NLO chiral perturbation theory applies. However, such a statement may depend sensitively on the observable and in this respect F_K/F_π is rather special. It is an $SU(3)$ -flavor breaking ratio in which the sea quark contributions cancel at NLO. Moreover, the NLO expressions fit our results for this ratio very well with only two parameters, F_0 and L_5 ; the size of NLO corrections are perfectly reasonable, of order 20%; and the values of F_0 and

L_5 that we obtain are acceptable for a fit performed at this order ¹. In addition, omission of all $SU(3)$ fits would shift our final result for F_K/F_π by less than one quarter of our final error, and slightly reduce the systematic error.

Ad (ii): Given the previous discussion, it is clear that the heavy kaon $SU(2)$ framework of [16] is an interesting alternative, since it does not assume that $m_s/(4\pi F_0) \ll 1$, but rather treats the strange quark as a heavy degree of freedom, which is “integrated out”. Of course, while this may be a good approximation at the physical value of m_{ud} , where $m_{ud}/m_s \ll 1$, it may break down for larger values, when $m_{ud} \lesssim m_s$, as is the case for our more massive points.

What is needed for our analysis is Eq. (53) of [16] for the pion mass dependence of F_K , together with the standard $SU(2)$ formula for the mass dependence of F_π [21]. In these expressions, every low-energy constant bears an implicit m_s dependence which can be written as a power series expansion in $m_s - m_s^{\text{phys}}$ about the physical point. In practice we are only sensitive to the m_s dependence of the LO term. Thus, we can express the ratio as

$$\frac{F_K}{F_\pi} = \frac{\bar{F}}{F} \left\{ 1 + \alpha \frac{m_s - m_s^{\text{phys}}}{\mu_{\text{QCD}}} \right\} \frac{1 - \frac{3}{8} \frac{M_\pi^2}{(4\pi F)^2} \log\left(\frac{M_\pi^2}{\Lambda^2}\right)}{1 - \frac{M_\pi^2}{(4\pi F)^2} \log\left(\frac{M_\pi^2}{\Lambda^2}\right)}, \quad (4)$$

where F, \bar{F} denote the two-flavor chiral limit of the pion and kaon decay constant, respectively, while $\Lambda, \bar{\Lambda}$ are the energy scales associated with the respective LECs ². In (4), μ_{QCD} is a typical hadronic energy scale.

This expression for F_K/F_π has five m_s -independent parameters ($\bar{F}, F, \alpha/\mu_{\text{QCD}}, \Lambda, \bar{\Lambda}$), four if the ratio is expanded and only NLO terms are kept ($\bar{F}, F, \alpha/\mu_{\text{QCD}}, \Lambda^{3/4}/\bar{\Lambda}^2$). We find that the former leads to unstable fits and thus do not use it in our analysis. One of the ways that we use to estimate possible contributions of higher order terms (see Sec. 2.5), is to consider two $SU(2)$ χ PT expressions, which are equivalent to (4) at NLO: the one, already discussed, obtained by fully expanding (4) to NLO and the other obtained by expanding the inverse of (4) to NLO. For reasons similar to those discussed under (i), we leave the determination of the LECs, which appear at NLO in Eq. (4), for future investigation.

In order to use the parameterization (4), one has to give a definition of $m_s - m_s^{\text{phys}}$. $SU(3)$ χ PT, together with Fig. 1 and the discussion surrounding it, suggests that $([2M_K^2 - M_\pi^2] - [\dots]_{\text{phys}})/\mu_{\text{QCD}} \propto (m_s - m_s^{\text{phys}})[1 + O(m_s - m_s^{\text{phys}})]$, up to negligible, physical, m_{ud} and m_{ud}^{phys} corrections, in the range of quark masses covered in our simulations. Thus, we use this difference of meson masses squared as a measure of $m_s - m_s^{\text{phys}}$.

Ad (iii): Both two and three flavor chiral perturbation theory are expansions about a singular point, $(m_{ud}, m_s) = (0, 0)$ in the case of $SU(3)$ and $(m_{ud}, m_s) = (0, m_s^{\text{phys}})$ in the case of $SU(2)$. However, here we are interested in the physical mass point, $(m_{ud}^{\text{phys}}, m_s^{\text{phys}})$, which is nearer the region in which we have lattice results than it is to either singular point. Thus, it makes sense to consider an expansion about a regular point which encompasses both the lattice results and the physical point [4]. As discussed above, the data at two lattice spacings ($\beta = 3.3$ and $\beta = 3.7$) have been generated at a fixed value of am_s , and the data at $\beta = 3.57$ can easily be interpolated to a fixed am_s . On the other hand, an extrapolation is needed in m_{ud} . It is

¹Note that the ratio F_K/F_π is not well suited for a determination of F_0 and L_5 . In this ratio, the LO LEC F_0 only appears at NLO where its value becomes highly correlated with that of L_5 . A serious determination of these constants would actually require a dedicated study which is beyond the scope of this paper.

²In the standard $SU(2)$ framework the former is usually denoted Λ_4 , since it is associated with l_4 [21].

natural to consider the following expansion parameters

$$\Delta_\pi = \left[M_\pi^2 - \frac{1}{2}(M_\pi^{\text{phys}})^2 - \frac{1}{2}(M_\pi^{\text{cut}})^2 \right] / \mu_{\text{QCD}}^2 \quad (5)$$

$$\Delta_K = \left[M_K^2 - (M_K^{\text{phys}})^2 \right] / \mu_{\text{QCD}}^2 \quad (6)$$

with μ_{QCD} as above and M_π^{cut} the heaviest pion mass included in the fit. The discussion in [4] suggests that the mass dependence of F_K/F_π in our ensembles and at the physical mass point can be described by a low order polynomial in these variables, leading to the ‘‘Taylor’’ or ‘‘flavor’’ ansatz

$$\frac{F_K}{F_\pi} = A_0 + A_1\Delta_\pi + A_2\Delta_\pi^2 + B_1\Delta_K. \quad (7)$$

One of the ways that we use to estimate possible contributions of higher order terms (see Sec.2.5), is to consider the same functional form for F_π/F_K . Thus, we consider two flavor ansaetze.

There are, of course, many possible variants of these ansaetze. For instance, Δ_K in Eq.(6) could be defined in terms of M_K instead of M_K^2 . One could also enforce $SU(3)$ flavor symmetry, i.e. $F_K/F_\pi = 1$ when $m_{ud} = m_s$. This could be done, for instance, with an expansion of the form $F_K/F_\pi = 1 + (M_K^2 - M_\pi^2) \times [\text{polynomial in } \Delta_\pi \text{ and } \Delta_K]$. However, the expansion of Eq.(7) provides a better description of our data than the alternatives that we have tried.

2.3 Continuum limit

To maximize the use of our data, we combine the continuum extrapolation with our interpolations and extrapolations to the physical strange and up-down quark mass point. As mentioned above, F_K/F_π is an $SU(3)$ -flavor breaking ratio, so that cutoff effects must be proportional to $m_s - m_{ud}$. Although [9] suggests that they are quadratic in a , our action is formally only improved up to $O(a\alpha_s)$ and we cannot exclude, a priori, the presence of linear discretization errors. Moreover, the effects are small enough that, despite a factor of almost two in lattice spacing, we cannot distinguish a from a^2 in our data. Thus, in our analysis, we consider three possibilities: no cutoff effects; cutoff effects of the form $a(m_s - m_{ud})$, and cutoff effects proportional to $a^2\mu_{\text{QCD}}(m_s - m_{ud})$. Again, μ_{QCD} is a typical hadronic energy scale.

In the case of $SU(3)$ χ PT, the cutoff effects can be accounted for by adding

$$\left. \frac{F_K}{F_\pi} \right|_{\text{c.o.}} = c \times \begin{cases} a(M_K^2 - M_\pi^2)/\mu_{\text{QCD}} \\ \text{or} \\ a^2(M_K^2 - M_\pi^2) \end{cases} \quad (8)$$

to the functional forms for the mass dependence of F_K/F_π given in the previous section. Here c is the relevant parameter.

In the usual power counting scheme of $SU(3)$ Wilson χ PT, in which $O(a) = O(m_q)$ [22], the cutoff effects considered in (8) are NNLO in the $O(a)$ case and even N³LO for those proportional to a^2 . This should be compared to the physical contributions to the deviation of F_K/F_π from 1, which are NLO. Thus, these cutoff effects are small parametrically and, as we will see below, they are also small numerically. In fact, they are consistent with zero within our statistical errors. Clearly then, any reasonable parameterization of these small $SU(3)$ -flavor breaking, cutoff effects is sufficient for our purposes. Thus, we use the parametrizations of Eq.(8) to subtract them, also in the context of $SU(2)$ χ PT and flavor expansions.

2.4 Infinite volume limit

The finite spatial size L of the box affects masses and decay constants of stable states in a manner proportional to $\exp(-M_\pi L)$ [23]. In our simulations the bound $M_\pi L \gtrsim 4$ is maintained. It turns out that the sign of the shift is the same for both decay constants so that such effects partly cancel in the ratio. In chiral perturbation theory to 1-loop order, $F_\pi(L)/F_\pi$ has been calculated in [24] and $F_K(L)/F_K$ in [25]. At the 2-loop level, both ratios have been determined in [26]. The generic formulae take the form

$$\frac{F_K(L)}{F_K} = 1 + \sum_{n=1}^{\infty} \frac{m(n)}{\sqrt{n}} \frac{1}{M_\pi L} \frac{F_\pi}{F_K} \frac{M_\pi^2}{(4\pi F_\pi)^2} \left[I_{F_K}^{(2)} + \frac{M_K^2}{(4\pi F_\pi)^2} I_{F_K}^{(4)} + \dots \right] \quad (9)$$

$$\frac{F_\pi(L)}{F_\pi} = 1 + \sum_{n=1}^{\infty} \frac{m(n)}{\sqrt{n}} \frac{1}{M_\pi L} \frac{1}{1} \frac{M_\pi^2}{(4\pi F_\pi)^2} \left[I_{F_\pi}^{(2)} + \frac{M_\pi^2}{(4\pi F_\pi)^2} I_{F_\pi}^{(4)} + \dots \right] \quad (10)$$

with $m(n)$ tabulated in [26]. With $I_{F_\pi}^{(2)} = -4K_1(\sqrt{n} M_\pi L)$ and $I_{F_K}^{(2)} = -\frac{3}{2}K_1(\sqrt{n} M_\pi L)$, where $K_1(\cdot)$ is a Bessel function of the second kind, one obtains the compact 1-loop expression [26]

$$\frac{F_K(L)}{F_\pi(L)} = \frac{F_K}{F_\pi} \left\{ 1 + \left[4 - \frac{3F_\pi}{2F_K} \right] \sum_{n=1}^{\infty} \frac{m(n)}{\sqrt{n}} \frac{1}{M_\pi L} \frac{M_\pi^2}{(4\pi F_\pi)^2} K_1(\sqrt{n} M_\pi L) \right\} \quad (11)$$

which is readily evaluated. On the other hand, the expressions $I_{F_K}^{(4)}$, $I_{F_\pi}^{(4)}$ in the 2-loop part are more cumbersome to deal with. Since finite-volume effects are independent of cutoff effects (see e.g. the discussion in [26]), we choose to first correct the data for finite volume effects before we actually perform the global fit (see below). The masses of the mesons are also corrected for finite volume effects according to [26].

To estimate the error associated with the finite volume effects, the difference between the 1-loop shift of F_K/F_π and the corrected value of F_K/F_π using only the expression for F_π (that should be an upper bound on the finite volume correction), is used as a measure of the uncertainty of the correction (see Sec. 2.5). In our final analysis, the finite volume shift is smaller than the statistical error in most of our ensembles.

2.5 Fitting strategy and treatment of theoretical errors

Our goal is to obtain F_K/F_π at the physical point, in the continuum and in infinite volume. To this end we perform a global fit which simultaneously extrapolates or interpolates $M_\pi^2 \rightarrow M_\pi^2|_{\text{phys}}$, $M_K^2 \rightarrow M_K^2|_{\text{phys}}$ and $a \rightarrow 0$, after the data have been corrected for very small finite volume effects, using the two-loop chiral perturbation theory results discussed above. To assess the various systematic uncertainties associated with our analysis, we consider a large number of alternative procedures.

To estimate the systematic uncertainty associated with setting the scale, we have repeated the analysis setting the scale with the Ξ and the Ω .

To estimate the possible contributions of excited states to the correlators used, we repeat our analysis using a total of 18 different time intervals: $t_{\text{min}}/a = 5$ or 6, for $\beta = 3.3$; 7, 8 or 9, for $\beta = 3.57$; 10, 11 or 12 for $\beta = 3.7$. All of these intervals are chosen so that the correlation functions are strongly dominated by the ground state. However, the intervals which begin at earlier times may receive some small contamination from excited states.

Uncertainties associated with the necessary extrapolation to the physical up and down quark-mass point are assessed by varying the functional form used as well as by varying the range of pion masses considered. As discussed in Sec. 2.2, we consider 3 forms based on the NLO $SU(3)$ formula of Eq. (2), 2 forms based on the NLO $SU(2)$ expression of Eq. (4), and 2 flavor ansaetze, based on Eq. (7). Moreover, we impose 2 cuts on the pion mass: $M_\pi < 350$ MeV and 460 MeV.

Our results for F_K/F_π display a small dependence on lattice spacing. As described in Sec. 2.3, to estimate the systematic associated with the continuum extrapolation we consider fits with and without $O(a^2)$ and $O(a)$ Symanzik factors.

All of this amounts to performing $2 \cdot 18 \cdot 7 \cdot 2 \cdot 3 = 1512$ alternative analyses. The central value obtained from each procedure is weighted with the quality of the (correlated) fit to construct a distribution. The median and the 16-th/84-th percentiles yield the final central value and the systematic error associated with possible excited state contributions, scale setting, and the chiral and continuum extrapolations. To obtain the final systematic error of our computation, we add a finite-volume uncertainty in quadrature to the error already obtained. This finite-volume uncertainty is given by the weighted (with the quality of the fit) standard deviation of our final central value and the ones obtained repeating the whole procedure with finite-volume effects subtracted at one loop and the upper bound computed as the 2 loop correction in F_π only. We do not include these two alternative options in the set of procedures which yield our final central value because we know, a priori, that the two-loop expressions of [26] are more accurate than the one-loop ones. To determine the statistical error, the whole procedure is bootstrapped (with 2000 samples) and the variance of the resulting medians is computed.

There is a final source of theoretical error which we wish to comment on: the one associated with the fact that our calculation is performed with $m_u=m_d$ and in the absence of electromagnetism. As discussed in the Introduction, we correct for these effects at leading order, up to a few per mil uncertainties. The latter have a negligible effect on F_K/F_π . One also expects direct isospin violation in F_K/F_π . These were found to be negligible in [11].

Having estimated the total systematic error, it is interesting to decompose it into its individual contributions. By construction, the contribution from the uncertainty in the finite-volume corrections is already known. To quantify the other contributions, we construct a distribution for each of the possible alternative procedures corresponding to the source of theoretical error under investigation. These distributions are obtained by varying over all of the other procedures and weighing the results by the total fit quality. Then, we compute the medians and average fit qualities of these distributions. Clearly the spread of the medians measure the uncertainty associated with the specific source of error. We use the standard deviation of these medians weighted by the average fit quality as an estimate of the error under consideration.

A “snapshot” fit (with a specific choice for the time intervals used in fitting the correlators, scale setting, pion mass range) can be seen in Fig. 2. To avoid the complications of a multi-dimensional plot, the extrapolation is shown as a function of the pion mass only. The data have been corrected for the deviation of the simulated m_s from m_s^{phys} . In other words, what is shown is $\text{data}(M_\pi^2, 2M_K^2 - M_\pi^2) - \text{fit}(M_\pi^2, 2M_K^2 - M_\pi^2) + \text{fit}(M_\pi^2, [2M_K^2 - M_\pi^2]_{\text{phys}})$. The figure shows one flavor fit with no cutoff effects. We emphasize that χ^2/dof for our correlated fits are close to one.

Fig. 3 shows the distribution of our 1512 alternative fitting procedures. As can be seen, the use of different formulas to extrapolate to the physical point only increases the systematic error. This is also true for the other sources of systematic error: scale setting, time intervals for

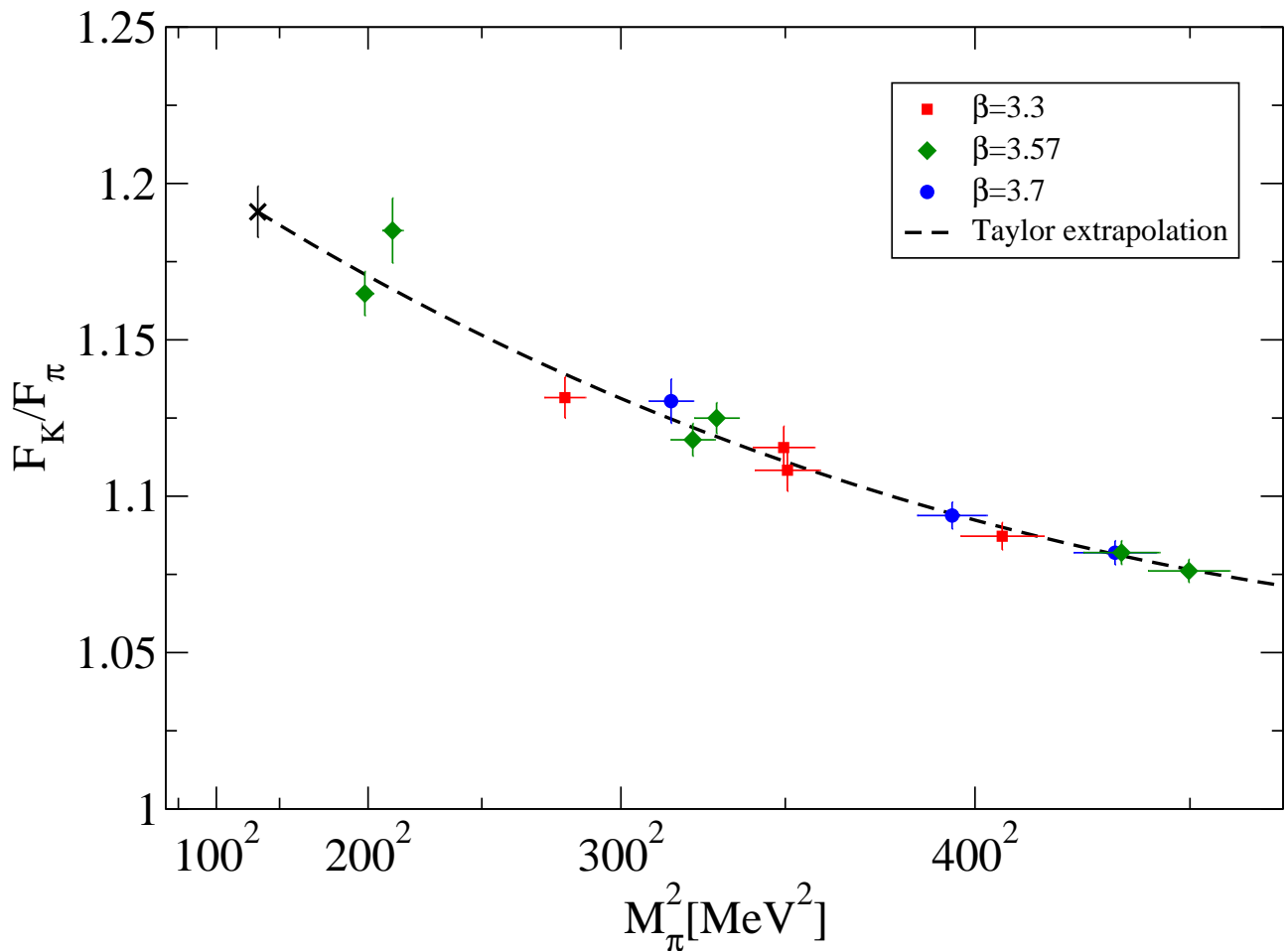


Figure 2: *Extrapolation of the lattice data to the physical point for a particular choice of two-point function fits ($t_{\min}/a = 6, 8, 11$ for $\beta = 3.3, 3.57, 3.7$, respectively), mass cut ($M_\pi < 460$ MeV) and using the Ξ to set the scale. The plot shows one (of the 21) fits used to estimate the uncertainty associated with the functional form used for the mass extrapolation. The data have been slightly adjusted to the physical strange quark mass, as well as corrected for tiny finite-volume effects (see text for details).*

the fit to the correlators, pion mass ranges and cutoff effects. The figure also shows our final result with the total final error.

3 Results and discussion

Following the procedure outlined above, our final result is

$$\left. \frac{F_K}{F_\pi} \right|_{\text{phys}} = 1.192(7)_{\text{stat}}(6)_{\text{syst}} \quad \text{or} \quad \left. \frac{F_\pi}{F_K} \right|_{\text{phys}} = 0.839(5)_{\text{stat}}(4)_{\text{syst}} \quad (12)$$

at the physical point, where all sources of systematic error have been included. Tab. 2 gives a breakdown of the systematic error according to the various sources. We conclude that our main source of systematic error comes from the chiral extrapolation (functional form and pion mass range), followed by cut-off effects.

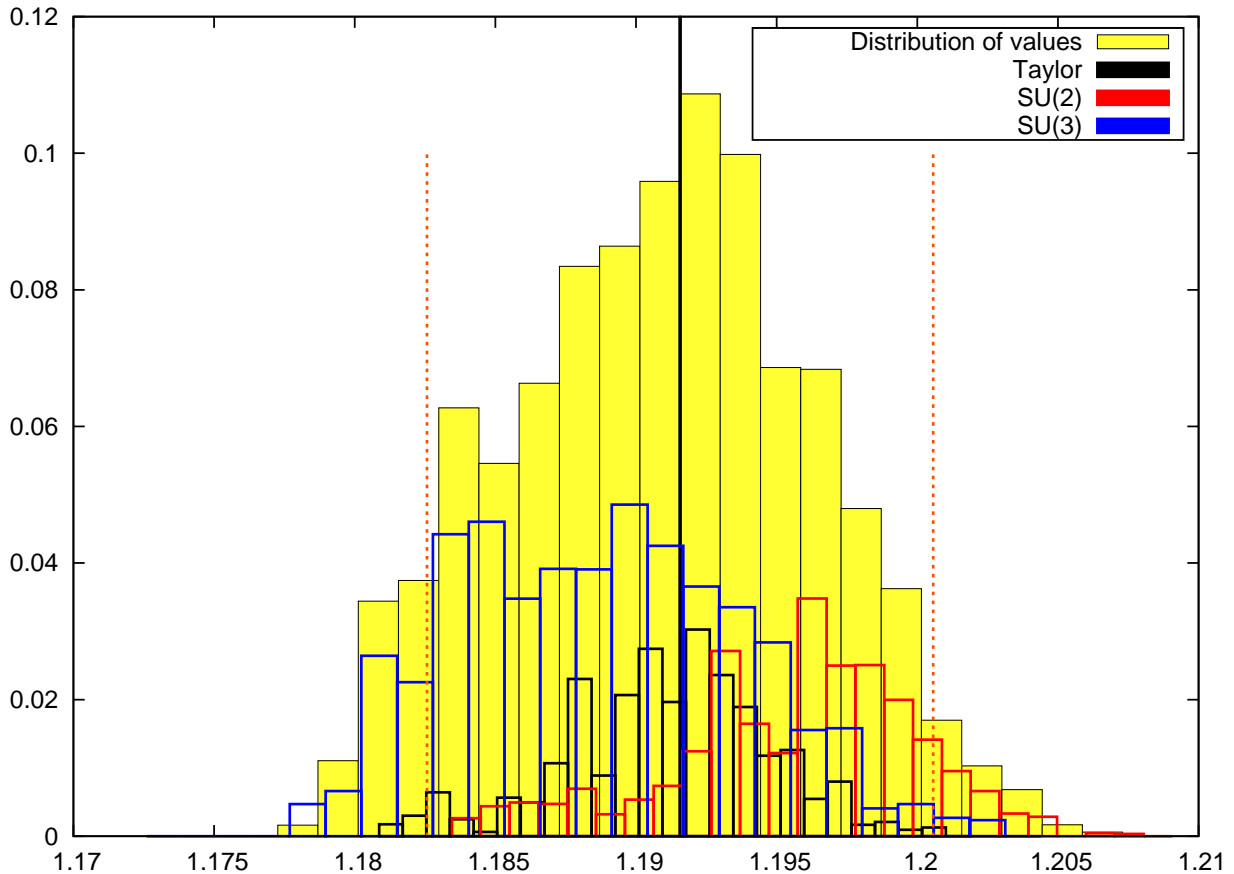


Figure 3: Distribution of final values for F_K/F_π . The large background distribution represents the values of F_K/F_π obtained with different extrapolation formulas, pion mass cuts, parameterization of cutoff effects, time intervals and different methods to set the scale. Also shown is the final result (solid vertical line) and final systematic error interval (dashed vertical lines), which includes the finite volume error estimate. The smaller distributions group the values according to the chiral formula used for the extrapolation. The error associated with the chiral extrapolation is computed as the weighted (by total fit quality) standard deviations of the medians of the grouped distributions.

In the same manner we may read off from our fits that the value in the 2-flavor chiral limit

$$\left. \frac{F_K}{F_\pi} \right|_{m_{ud}=0, m_s \text{ phys}} = 1.217(10)_{\text{stat}}(9)_{\text{syst}} \quad \text{or} \quad \left. \frac{F_\pi}{F_K} \right|_{m_{ud}=0, m_s \text{ phys}} = 0.821(7)_{\text{stat}}(6)_{\text{syst}} \quad (13)$$

differs by about 2% from the physical value, though with larger uncertainties. Upon combining this ratio in the $SU(2)$ chiral limit with the phenomenological value $F = \lim_{m_{ud} \rightarrow 0} F_\pi = 86.2(5)$ MeV [27], we obtain $\lim_{m_{ud} \rightarrow 0} F_K = 104.9(1.3)$ MeV at fixed physical m_s .

In Fig. 4 a survey of recent determinations of F_K/F_π in unquenched QCD simulations is presented. These include results by JLQCD [10], MILC [11, 12], NPLQCD [13], HPQCD/UKQCD [14], ETM [15] RBC/UKQCD [16], PACS-CS [17], and Aubin et al. [18]. It is worth noting that these results show a good overall consistency when one excludes the outlier point of [10].

The result by HPQCD/UKQCD remains the one with the highest claimed accuracy. Our precision is similar to that of another state-of-the-art calculation, the one by MILC. Given

Source of systematic error	error on F_K/F_π
Chiral Extrapolation:	
- Functional form	3.3×10^{-3}
- Pion mass range	3.0×10^{-3}
Continuum extrapolation	3.3×10^{-3}
Excited states	1.9×10^{-3}
Scale setting	1.0×10^{-3}
Finite volume	6.2×10^{-4}

Table 2: *Breakdown of the total systematic error on F_K/F_π into its various components, in order of decreasing importance.*

that we reach smaller pion masses, that more generally we explore a large range of simulation parameters which allows us to control all sources of systematic error, that we use an action with a one-to-one matching of lattice-to-continuum flavor and that we avoid the specifics of a partially quenched framework, our result solidifies the claim that F_K/F_π is known to better than 1%. Moreover, agreement between such different approaches can only bolster confidence in the reliability of lattice calculations per se.

4 Update on $|V_{us}|$ and check of CKM unitarity relation

With the result (12) in hand, we can now focus on CKM matrix elements. In this respect there are two options – we may *assume* the SM (and hence CKM unitarity) and determine $|V_{ud}|$ and $|V_{us}|$, or we may use phenomenological input on $|V_{ud}|$ to derive $|V_{us}|$ and hence *test* CKM unitarity (under the assumption of quark-flavor universality) in a model-independent way.

The first step, needed in either case, is to simplify Marciano’s Eq. (1). The most recent update of the Flavianet kaon working group is [2]

$$\frac{|V_{us}|}{|V_{ud}|} \frac{F_K}{F_\pi} = 0.27599(59) . \quad (14)$$

Combining this with our result (12) yields the ratio

$$|V_{us}|/|V_{ud}| = 0.2315(19) . \quad (15)$$

Now for the two options. If we assume unitarity, (15) and $|V_{ub}| = (3.93 \pm 0.36) 10^{-3}$ [7] imply

$$|V_{ud}| = 0.97422(40) , \quad |V_{us}| = 0.2256(17) . \quad (16)$$

On the other hand, if we combine (15) with the most precise information on the first CKM matrix element available today, $|V_{ud}| = 0.97425(22)$ [8], we obtain (again)

$$|V_{us}| = 0.2256(18) . \quad (17)$$

Similarly, by also including the above mentioned result for $|V_{ub}|$ we find

$$|V_{ud}|^2 + |V_{us}|^2 + |V_{ub}|^2 = 1.0001(9) . \quad (18)$$

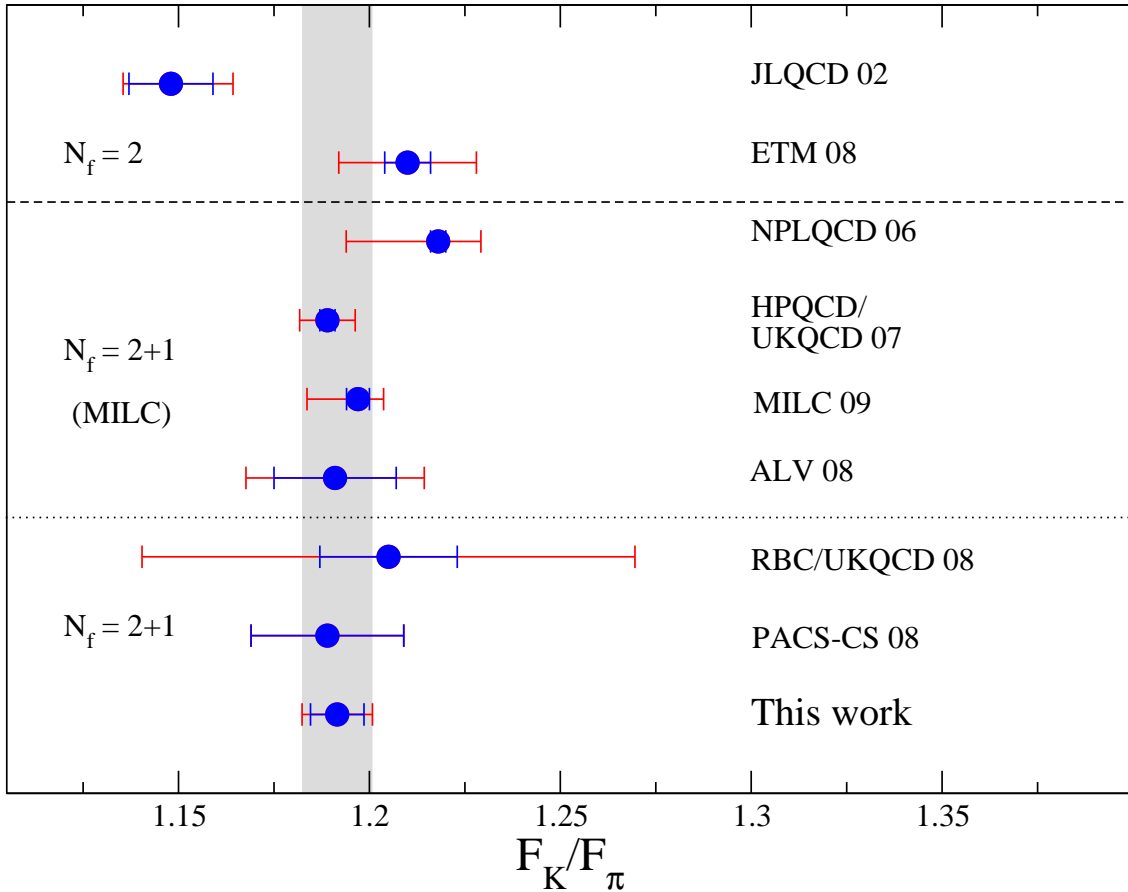


Figure 4: *Our result (12) compared to previous unquenched lattice QCD calculations. The two error bars refer to the statistical and to the combined statistical and systematic uncertainties, respectively. The top two results were obtained with $N_f = 2$ simulations. The next four were computed on $N_f = 2 + 1$ MILC configurations. RBC/UKQCD and PACS-CS determinations were obtained on distinct $N_f = 2 + 1$ ensembles.*

With the first-row unitarity relation (which is genuine to the CKM paradigm) being so well observed, there is no support for “beyond the Standard Model” physics contributions to these processes. Of course, with substantially improved precision on both the theoretical and the experimental side, this might change in the future.

5 Summary

Based on a series of 18 large scale lattice computations the ratio F_K/F_π has been determined in $N_f = 2 + 1$ flavor QCD at the physical mass point, in the continuum and in infinite volume. The overall precision attained is at the 1% level, with statistical and systematic errors being of similar magnitude. The systematic error, in turn, splits into uncertainties arising from the extrapolation to the physical pion mass, to the continuum, to possible excited state contributions and to finite volume effects. We find that the main source of systematic error comes from the extrapolation to the physical point. In this respect it is useful that our simulations cover the pion mass range down to about 190 MeV, with small cutoff effects and volumes large enough

to maintain the bound $M_\pi L \gtrsim 4$.

Following Marciano's suggestion [6], we use our result (12) for F_K/F_π to obtain the value (15) for $|V_{us}|/|V_{ud}|$ and subsequently $|V_{us}|$. In turn, these results are used to test first row unitarity, which we find is satisfied at the 1 per mil level, thereby imposing interesting constraints on “new physics” scenarios (see e.g. [2]).

Acknowledgments: Computations were performed on Blue Gene supercomputers at FZ Jülich and IDRIS (GENCI), as well as on clusters at Wuppertal and CPT. This work is supported in part by the U.S. Department of Energy under Grant No. DE-FG02-05ER25681, EU grant I3HP, OTKA grant AT049652, DFG grant FO 502/1-2, SFB/TR-55, EU RTN contract MRTN-CT-2006-035482 (FLAVIANet) and by the CNRS's GDR grant n° 2921 and PICS grant n° 4707.

References

- [1] See e.g. the working group reports from the workshop “Flavour in the Era of the LHC” (Nov 7, 2005 - Mar 28, 2007) held at CERN: F. del Aguila *et al.*, Eur. Phys. J. C **57**, 183 (2008) [arXiv:0801.1800, hep-ph], M. Artuso *et al.*, *ibid.* C **57**, 309 (2008) [arXiv:0801.1833, hep-ph], M. Raidal *et al.*, *ibid.* C **57**, 13 (2008) [arXiv:0801.1826, hep-ph].
- [2] M. Antonelli *et al.* [FlaviaNet Working Group on Kaon Decays], Nucl. Phys. Proc. Suppl. **181-182**, 83 (2008) [arXiv:0801.1817, hep-ph].
- [3] A. Jüttner, PoS **LAT2007**, 014 (2007) [arXiv:0711.1239, hep-lat].
- [4] L. Lellouch, PoS **LAT2008**, 015 (2009) [arXiv:0902.4545, hep-lat].
- [5] V. Lubicz, Lattice 2009 plenary talk.
- [6] W. J. Marciano, Phys. Rev. Lett. **93**, 231803 (2004) [hep-ph/0402299].
- [7] C. Amsler *et al.* [Particle Data Group], Phys. Lett. B **667**, 1 (2008).
- [8] J. C. Hardy and I. S. Towner, Phys. Rev. C **79**, 055502 (2009) [arXiv:0812.1202, nucl-ex].
- [9] S. Dürr *et al.* [Budapest-Marseille-Wuppertal Collab.], Phys. Rev. D **79**, 014501 (2009) [arXiv:0802.2706, hep-lat].
- [10] S. Aoki *et al.* [JLQCD Collab.], Phys. Rev. D **68**, 054502 (2003) [hep-lat/0212039].
- [11] C. Aubin *et al.* [MILC Collab.], Phys. Rev. D **70**, 114501 (2004) [hep-lat/0407028].
- [12] A. Bazavov *et al.* [MILC Collab.], arXiv:0903.3598 [hep-lat].
- [13] S. R. Beane, P. F. Bedaque, K. Orginos and M. J. Savage [NPLQCD Collab.], Phys. Rev. D **75**, 094501 (2007) [hep-lat/0606023].
- [14] E. Follana, C. T. H. Davies, G. P. Lepage and J. Shigemitsu [HPQCD Collab.], Phys. Rev. Lett. **100**, 062002 (2008) [arXiv:0706.1726, hep-lat].
- [15] B. Blossier *et al.* [ETM Collab.], JHEP **0907**, 043 (2009) [arXiv:0904.0954, hep-lat].
- [16] C. Allton *et al.* [RBC/UKQCD Collab.], Phys. Rev. D **78**, 114509 (2008) [arXiv:0804.0473, hep-lat].
- [17] S. Aoki *et al.* [PACS-CS Collab.], Phys. Rev. D **79**, 034503 (2009) [arXiv:0807.1661, hep-lat].
- [18] C. Aubin, J. Laiho and R. S. Van de Water, arXiv:0810.4328 [hep-lat].
- [19] S. Dürr *et al.*, Science **322**, 1224 (2008) [arXiv:0906.3599, hep-lat].
- [20] J. Gasser and H. Leutwyler, Nucl. Phys. B **250**, 465 (1985).
- [21] J. Gasser and H. Leutwyler, Annals Phys. **158**, 142 (1984).
- [22] O. Bär, G. Rupak and N. Shores, Phys. Rev. D **70**, 034508 (2004) [hep-lat/0306021].
- [23] M. Lüscher, Commun. Math. Phys. **104**, 177 (1986).
- [24] J. Gasser and H. Leutwyler, Phys. Lett. B **184**, 83 (1987).
- [25] D. Becirevic and G. Villadoro, Phys. Rev. D **69**, 054010 (2004) [hep-lat/0311028].
- [26] G. Colangelo, S. Dürr and C. Haefeli, Nucl. Phys. B **721**, 136 (2005) [hep-lat/0503014].
- [27] G. Colangelo and S. Dürr, Eur. Phys. J. C **33**, 543 (2004) [hep-lat/0311023].